2024 IEEE Transportation Electrification Conference and Expo (ITEC) | 979-8-3503-1766-4/24/$31.00 ©2024 IEEE | DOI: 10.1109/ITEC60657.2024.10599067

A Novel Four Switch Transformerless Inverter with Step Up/Down Capability for PV Fed Grid Connected Systems

Phani Kumar Chamarthi[1], Ali Moghassemi[1,*], S M Imrat Rahman[1], Laxman Timilsina[1], Okan Ciftci[1], Elutunji Buraimoh[1], Gokhan Ozkan[1,2], Behnaz Papari[1,3], Christopher S. Edrington[1]
Email: phanikumareee@gmail.com, {amoghas*,smimrar,ltimils,ociftci, eburaim,gokhano,bpapari,cedring}@clemson.edu
[1]Holcombe Department of Electrical and Computer Engineering, Clemson University, Clemson 29634, SC, USA
[2]Dominion Energy Innovation Center, Clemson University, North Charleston 29405, SC, USA
[3]Department of Automotive Engineering, Clemson University, Greenville 29607, SC, USA

***Abstract*—This paper presents a novel four-switch transformerless inverter (FSTI) topology for 1-ø grid-connected solar photovoltaic applications with reactive power capability. This proposed FSTI steps up/down the output voltage while completely suppressing the leakage/parasitic currents. Further, this inverter topology supports the on/off-grid application where active/reactive power requirement is essential. In addition, the FSTI comprises of least active power devices, lower voltage and current stresses of power devices, appropriate THD in grid current and better efficiency. The FSTI performance is evaluated for the 1-ø grid connected system. The FSTI is modeled using small signal analysis for the grid-connected inverter's stable operation and fast response. The FSTI is validated on a 500VA laboratory prototype for input PV voltages of 100V, 180V and grid voltage of 110Vrms. The experimental results are in good agreement with the theoretical analysis, which verifies the practicality of the proposed inverter. The FSTI demonstrates the DC to AC power transfer while stepping up/down the inverter's output voltage with maximum efficiencies of 97% and 96% for the input voltages of 180V and 100V, respectively.**

Keywords—Solar PV, Transformerless Inverter, Total Harmonic Distortion, Efficiency, Reactive Power.

I. Introduction

A. Literature Review

Generally, transformerless PV inverters are higher in efficiency, lower in cost, and less in size and volume. But removing the transformer in the system will eliminate the galvanic isolation between the PV inverter and AC grid, which will introduce the leakage current into the grid, increase THD in grid current, increase power losses and may saturate the core of other distribution transformers in the power network which may increase safety issues further [1], [2]. These leakage currents are generated due to the variation in the voltage across parasitic capacitors that exists between the negative terminal of the PV source and grid neutral [3].

As per the standard IEC 62109-2-2011, if the leakage current goes beyond 0.03A, the PV inverter should be disconnected from the utility grid within 0.3 sec [4]. Nowadays, the usage of transformerless inverters for grid-integrated solar PV applications and new transformerless inverter topologies for reducing/eliminating leakage current has become of major interest to researchers. From [5], [6], the appropriate way out for eliminating the leakage current is a common ground transformerless inverter configuration.

Other than eliminating leakage currents, the additional essential features the grid integrated inverters must have:

- Capability to deliver reactive power to the utility grid as per the standard IEEE 1547-2018.
- Reduced power switch count, which lowers the system cost and power losses and enhances the inverter's efficiency.
- Step up/down the inverter's output voltage capability for a wide variation of input PV voltage.
- Lower voltage and current stresses of power devices.

Researchers in the past have come up with several common-ground inverters [7]-[16]. However, the introduced inverter topologies suffer from high power device count, inability to step the output voltage, and inability to absorb or inject reactive power into the utility grid. Authors in [17] and [18] have come up with low switch count common ground inverters; these inverter topologies also suffer from the inability to set the output voltage. The authors in [19] have come up with a transformerless inverter configuration with three switches. However, this topology produces less output voltage and is more sensitive to changes in the duty cycle. Hence, the application of inverters in [20]-[24] is restricted for off-grid applications due to their incapability to meet volt-var requirements as per standard IEEE 1547-2018.

So far in the literature, the transformerless inverters with both step-up/down capability and capability to supply reactive power are [21] and [22]. The inverters in [23] and [24] consist of seven and six power switches, respectively. The presence of a higher number of switches increases the difficulty in the implementation and development of control architecture. Furthermore, the gain in the output voltage of this inverter is twice the input voltage.

B. Contribution of the Paper

The main contribution of this paper is to introduce a new transformerless inverter topology that can step/down the output voltage and inject/receive reactive power to the utility grid with only four power switches. This proposed inverter is also easy to implement and has lower stress across power devices. Due to the lowest voltage stress across power devices compared to existing transformerless inverter topologies, this inverter uses lower-rated power devices, which improves the system's efficiency.

In brief, the proposed four-switch transformerless inverter (FSTI) is the first in the literature with the common ground feature, step-up/down capability and ability to supply/receive reactive power with lower voltage stress across power devices.

The paper is structured as follows. The configuration of the proposed FSTI, along with its most important working

979-8-3503-1766-4/24/$31.00 ©2024 IEEE

modes, are presented in Section 2. Section 3 discusses the modulation and control strategies along with key experimental results. The most important conclusions drawn from the proposed work are discussed in Section 4.

II. Proposed Four-Switch Transformerless Inverter Topology

A. Mathematical Model

Fig. 1 shows the configuration of the proposed four-switch transformerless inverter topology. This FSTI configuration is developed by merging the inverting and non-inverting Cuk converters. FSTI consists of four power switches S_1 to S_4, two inductors at the input (L_1 and L_2), five power diodes D_1 to D_5, two intermediate capacitors (C_1 and C_2), and one output inductor (L_3). It can be seen from Fig. 1 that the grid neutral and negative rail of the input PV source share a common connection, which suppresses the parasitic currents completely.

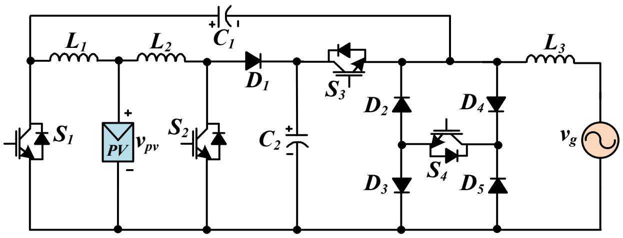

Fig. 1. Proposed common ground step up/down FSTI topology.

The important working modes of FSTI are shown in Figs. 2(a)-(d) corresponding to the grid's positive and negative half cycle. In any mode of operation, a maximum of two switches conduct out of four, operating only at the switching frequency. All switching states of FSTI with respect to the various working modes are provided in Table I.

TABLE I. Switches States Correspond to Various Modes

Operation of FSTI	Switches States (1=ON, 0=OFF)				Mode
	S_1	S_2	S_3	S_4	
$+V_e$ half cycle	0	1	1	0	I
	0	0	0	1	II
$-V_e$ half cycle	1	0	0	0	III
	0	0	0	1	IV

The modulation index (m_i) for the continuous conduction mode (CCM) and discontinuous conduction mode (DCM) for the proposed FSTI configuration by considering the input PV voltage and AC output voltages. In addition, the value of the modulation index varies with time due to the nature of the output voltage being AC.

The expression for the AC rms output voltage in CCM can be expressed as

$$V_{AC} = \frac{m_i}{1 - m_i} V_{PV} \quad (1)$$

By using (1), the peak value of the modulation index in CCM can be obtained as:

$$\hat{m}_i = \frac{V_{PV} + \hat{V}_{AC}}{\hat{V}_{AC}} \quad (2)$$

In addition, the expressions for ripple in the input inductors (L_1 and L_2) can be obtained as:

$$\Delta i_{L_1} = \left(\frac{V_{PV}}{f_S \times L_1}\right) m_i \quad (3\text{-a})$$

$$\Delta i_{L_2} = \left(\frac{V_{PV}}{f_S \times L_2}\right) m_i \quad (3\text{-b})$$

Where f_S is the switching frequency. The average current flowing through the input inductors (L_1 and L_2) during DCM can be given below.

$$I_{L_1} = \left(\frac{\hat{m}_i + {m_i}^+}{2}\right) \times \Delta i_{L_1} \quad (4\text{-a})$$

$$I_{L_2} = \left(\frac{\hat{m}_i + {m_i}^-}{2}\right) \times \Delta i_{L_2} \quad (4\text{-b})$$

Hence, the $(m_i)^+$ and $(m_i)^-$ during DCM are expressed as:

$${m_i}^+ = \frac{2 I_{L_1} f_S L_1}{\hat{m}_i V_{PV}} - \hat{m}_i \quad (5\text{-a})$$

$${m_i}^- = \frac{2 I_{L_2} f_S L_2}{\hat{m}_i V_{PV}} - \hat{m}_i \quad (5\text{-b})$$

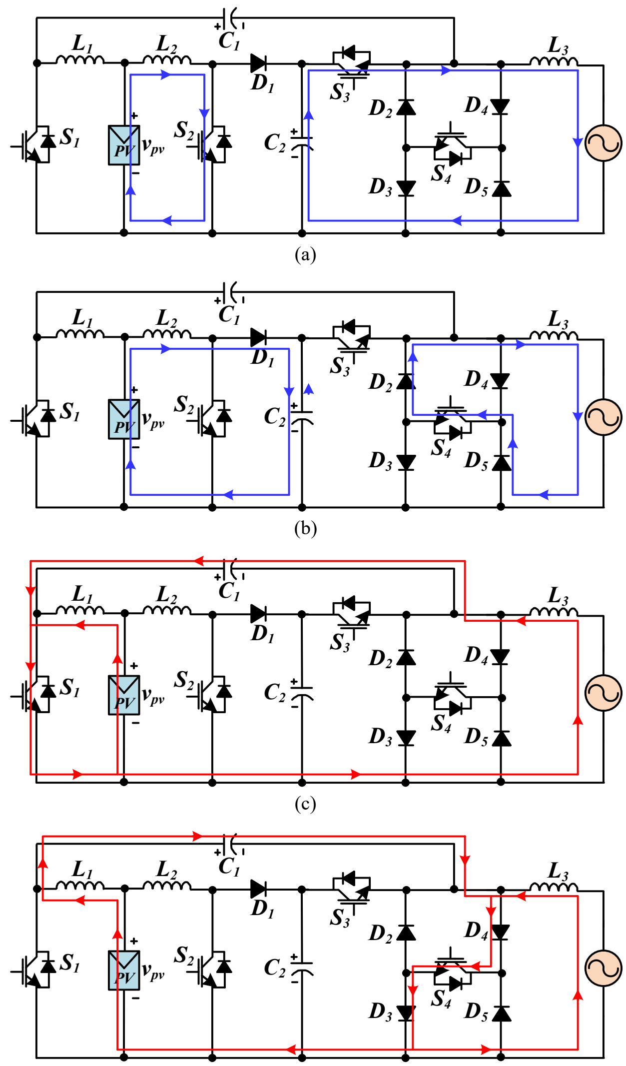

Fig. 2. The working modes of the proposed FSTI topology correspond to (a) & (b) +Ve half cycle; (c) & (d) -Ve half cycle.

By using (2), (4) and (5), the expressions for the peak value of the modulation index for positive and negative half cycles in DCM can be expressed as follows:

$$\hat{m}_i{}^{+} = \hat{m}_i{}^{-} = \frac{V_{PV} \times \hat{m}_i}{(\hat{V}_{AC} - V_{PV})} \tag{6}$$

B. Design of Passive Components

The grid's output inductor (L_3) is designed by considering the grid voltage and ripple in the inductor current. It can be expressed below:

$$L_3 \geq \frac{V_{AC} \times (1 - \hat{m}_i)}{f_S \times \Delta i_{AC}} \tag{7}$$

The L_1 and L_2 values can be computed by considering the DCM boundary condition. Therefore, by using (4) and (7), the expressions for L_1 and L_2 in DCM can be obtained as:

$$L_1 = L_2 \leq \frac{m_i \times V_{PV}}{2 \times f_S \times I_{L1}} \tag{8}$$

It can be observed that the voltage across the auxiliary capacitors C_1 and C_2 must be maintained constant in each switching cycle (T_s=$1/f_S$). Hence, the resonant frequency (w_r) of the output inductor (L_3), input inductor (L_1) and auxiliary capacitor (C_1) in the positive half cycle should be greater than the frequency of the grid (i.e. 50 Hz). Similarly, the resonant frequency between the L_3, C_2 and L_2 also should be greater than 50Hz. The expressions for auxiliary capacitors C_1 and C_2 can be expressed as given below:

$$C_1 = C_2 = \frac{1}{\omega_r^2 \times (L_3 + L_{1,2})} \tag{9}$$

For example, the FSTI configuration is having a switching frequency of 20kHz, L_1=L_2=117µH, V_{PV}=100V, V_{AC}=110rms, C_1=C_2= 75µF, and L_3=1mH.

C. Ratings of the Power Devices:

The average voltage across the power devices during the OFF state can be expressed below:

$$V_{S_1} = V_{C_1} + V_{PV} = \left(\frac{m_i}{1 - m_i} + 1\right) \times V_{PV} = \left(\frac{1}{1 - m_i}\right) \times V_{PV} \tag{10}$$

$$V_{S_2} = V_{C_2} + I_g = \left(\frac{1}{1 - m_i}\right) \times V_{PV} \tag{11}$$

$$V_{D_1} = 0 \tag{12}$$

$$V_{D_2} = V_{D_3} = V_{D_4} = V_{D_5} = \left(\frac{1}{1 - m_i}\right) \times V_{PV} \tag{13}$$

Also, the average current through diodes during the ON state can be expressed below:

$$I_{S_1} = I_{L_1} + I_g = \left(\frac{m_i}{1 - m_i} + 1\right) \times I_g = \left(\frac{1}{1 - m_i}\right) \times I_g \tag{14}$$

$$I_{S_2} = I_{L_2} + I_g = \left(\frac{m_i}{1 - m_i} + 1\right) \times I_g = \left(\frac{1}{1 - m_i}\right) \times I_g \tag{15}$$

$$I_{D_1} = \left(\frac{m_i}{1 - m_i}\right) \times I_g \tag{16}$$

$$I_{D_2} = I_{D_3} = I_{D_4} = I_{D_5} = \left(\frac{1}{1 - m_i}\right) \times I_g \tag{17}$$

The proposed FSTI configuration experiences lower power losses (i.e., switching and conduction) due to only two switches in conduction and three switches operating at high frequency in the positive cycle. In the negative half cycle, FSTI experiences even much lower losses than the positive half cycle because only one switch conducts any mode and only two switches operate at high frequency, as depicted in Figs. 2(a)-(d). Hence, the FSTI has incurred lower power losses among transformerless inverter topologies in the literature, which makes the proposed configuration a highly efficient and reliable way out for grid-connected solar PV applications. Further, the in-depth comparison is given in Table II to show the significance of the FSTI over other single stage transformerless inverters.

TABLE II. COMPARISON OF FSTI WITH EXISTING STEP-UP/DOWN TRANSFORMERLESS INVERTERS

Parameters	**FSTI**	**Ref [11]**	**Ref [12]**	**Ref [13]**
Number of switches	4	3	6	7
Number of diodes	5	3	2	3
Number of inductors	3	4	3	1
Number of capacitors	2	4	4	3
Total components	14	14	15	14
DC offset	No	Yes	Yes	No
% THD	2.9	4.5	<5	<5

III. MODULATION/CONTROL STRATEGIES AND KEY EXPERIMENTAL RESULTS

Fig. 3 shows the modulation/control technique introduced to control the proposed FSTI configuration. The modulation technique uses one absolute sine wave $|V_m sinwt|$ and one triangular waveform V_{tri}, as shown in Fig. 3(a). The comparison of $|V_m sinwt|$ and V_{tri} gives switching pulses to the various switches (S_1 to S_4) of the proposed FSTI configuration. To track the maximum available power from the input PV source and feed the maximum available power from PV to the grid, the closed-loop control technique of the proposed FSTI is shown in Fig. 3(b).

The grid-connected PV-fed FSTI system is validated on a laboratory prototype for a 500VA power rating. The system parameters of the experimental setup are provided in Table III. The important experimental waveforms, for example, current through grid (i_g), grid voltage (v_g), input inductor currents (i_{L1} and i_{L2}) and the voltage across auxiliary capacitors (v_{C1} and v_{C2}), are shown in Figs. 4(a)-(c). All experimental results corresponding to variations in the input voltages while injecting/absorbing reactive power to/from the utility grid will be discussed in future papers.

TABLE III. PARAMETERS OF EXPERIMENTAL STUDY

Parameter	**Value**
Power rating	500VA
Grid voltage	110V rms
Switching frequency	20kHz
Input voltage	100V
Input inductors (L_1 &L_2)	117µH
Intermediate capacitors (C_1 &C_2)	75µF
Output inductor (L_g)	1mH
Power switches	IHW25N120E1XKSA1
Power diodes	RHRP15120
DSP Controller	TMS320F28335

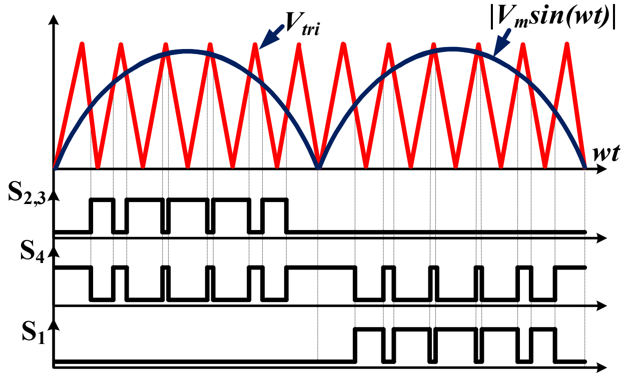

(a)

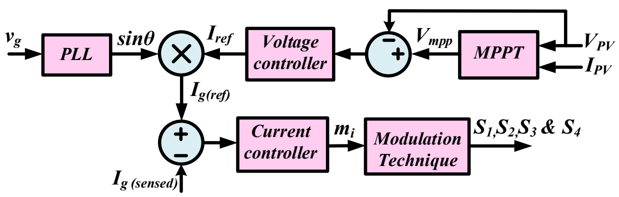

(b)

Fig. 3. Modulation and current control strategies of the proposed PV fed grid connected FSTI topology

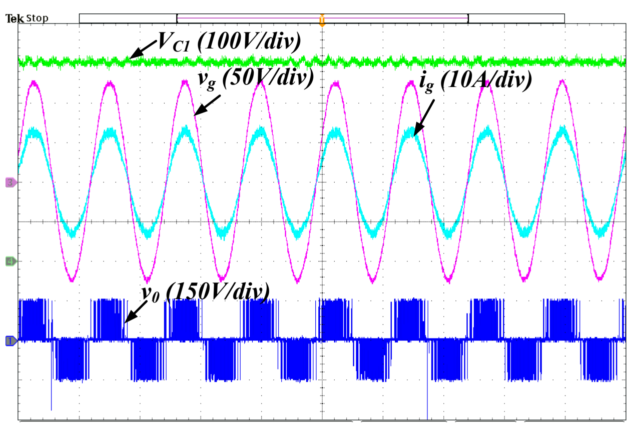

(a)

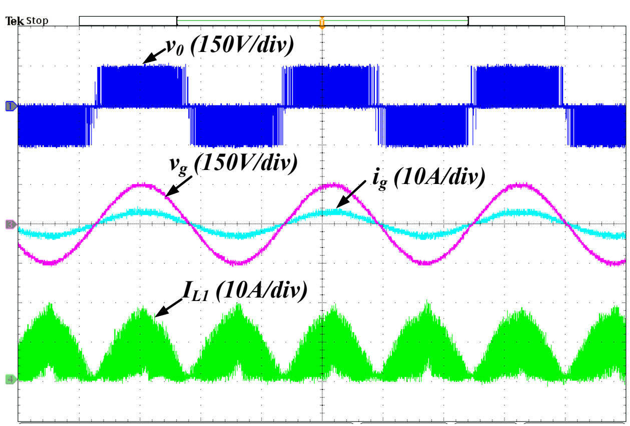

(b)

Fig. 4. Experimental waveforms of FSTI topology corresponding to current in input inductor (i_{L1}), output voltage (V_O), grid voltage (V_g), grid current (i_g) and the voltage across C_1.

IV. Conclusions and Future Work

In this paper a novel FSTI was introduced, studied, and verified through experimental analysis. From the experimental studies, it is evident that the proposed FSTI configuration suppresses/eliminates leakage current while stepping up/down output voltage and injecting/absorbing reactive power. In addition, the buck-boost nature of FSTI topology allowed us to track the input PV's maximum power point during a wide variation of weather conditions. It has also been observed from the experimental results that FSTI topology could feed a nice quality of current into the utility grid with a THD of 2.9%. It can be noted that the grid-connected FSTI was experimented with by considering a switching frequency of 20kHz. Currently several experimental studies of the proposed FSTI are in progress.

Acknowledgment

The authors would like to acknowledge the Warren H. Owen Distinguished Professorship Endowment for its support of the research effort.

References

[1] K. Alluhaybi, I. Batarseh and H. Hu, "Comprehensive Review and Comparison of Single-Phase Grid-Tied Photovoltaic Microinverters," in *IEEE Journal of Emerging and Selected Topics in Power Electronics*, vol. 8, no. 2, pp. 1310-1329, June 2020.

[2] T. H. Shahsavar *et al*., "A New Flying Capacitor-Based Buck–Boost Converter for Dual-Purpose Applications," in *IEEE Journal of Emerging and Selected Topics in Industrial Electronics*, vol. 4, no. 2, pp. 447-459, April 2023.

[3] Q. Yang, J. Yang and R. Li, "Analysis of Grid Current Distortion and Waveform Improvement Methods of Dual-Active-Bridge Microinverter," in *IEEE Transactions on Power Electronics*, vol. 38, no. 4, pp. 4345-4359, April 2023.

[4] Y. Chen, D. Xu and J. Xi, "Common-Mode Filter Design for a Transformerless ZVS Full-Bridge Inverter," in *IEEE Journal of Emerging and Selected Topics in Power Electronics*, vol. 4, no. 2, pp. 405-413, June 2016.

[5] R. Heidari, E. Adib, K. -I. Jeong and J. -W. Ahn, "Soft-Switched Boost–Cuk-Type High Step-Up Converter for Grid-Tied With Half-Bridge Inverter," in *IEEE Journal of Emerging and Selected Topics in Power Electronics*, vol. 11, no. 1, pp. 786-795, Feb. 2023.

[6] J. A. Flores and P. R. Rivera, "Single-Phase Grid-Connected MicroInverter for Low Power Photovoltaic Residential Applications," 2022 *IEEE ANDESCON*, Barranquilla, Colombia, 2022, pp. 1-6, November 2022.

[7] A. Kumar and P. Sensarma, "New Switching Strategy for Single-Mode Operation of a Single-Stage Buck–Boost Inverter," in *IEEE Transactions on Power Electronics*, vol. 33, no. 7, pp. 5927-5936, July 2018.

[8] J. F. Ardashir, M. Sabahi, S. H. Hosseini, F. Blaabjerg, E. Babaei and G. B. Gharehpetian, "A Single-Phase Transformerless Inverter With Charge Pump Circuit Concept for Grid-Tied PV Applications," in IEEE Transactions on Industrial Electronics, vol. 64, no. 7, pp. 5403-5415, July 2017.

[9] H. Xiao and S. Xie, "Leakage Current Analytical Model and Application in Single-Phase Transformerless Photovoltaic Grid-Connected Inverter," in *IEEE Transactions on Electromagnetic Compatibility*, vol. 52, no. 4, pp. 902-913, Nov. 2010.

[10] H. Tian, M. Chen, G. Liang and X. Xiao, "A Single-Phase Transformerless Common-Ground Type PV Inverter With Active Power Decoupling," in *IEEE Transactions on Industrial Electronics*, vol. 70, no. 4, pp. 3762-3772, April 2023.

[11] A. Sarikhani, M. M. Takantape and M. Hamzeh, "A Transformerless Common-Ground Three-Switch Single-Phase Inverter for Photovoltaic Systems," in *IEEE Transactions on Power Electronics*, vol. 35, no. 9, pp. 8902-8909, Sept. 2020.

[12] P. K. Chamarthi, M. S. El Moursi, V. Khadkikar, K. H. A. Hosani and T. H. M. El-Fouly, "Novel Step-Up

Transformerless Inverter Topology for 1-Φ Grid-Connected Photovoltaic System," in *IEEE Transactions on Industry Applications*, vol. 57, no. 3, pp. 2801-2815, May-June 2021.

[13] N. Vosoughi, S. H. Hosseini and M. Sabahi, "A New Single-Phase Transformerless Grid-Connected Inverter With Boosting Ability and Common Ground Feature," in *IEEE Transactions on Industrial Electronics*, vol. 67, no. 11, pp. 9313-9325, Nov. 2020.

[14] A. Kirubakaran, R. Barzegarkhoo and M. Liserre, "A New Common Ground Single-Phase Transformerless Five-Level Inverter for Photovoltaic Applications," *2024 Third International Conference on Power, Control and Computing Technologies (ICPC2T)*, Raipur, India, 2024, pp. 218-222.

[15] E. Demirkutlu and I. Iskender, "Transformerless Single-Phase Buck–Boost Inverter Decoupled From the Midpoint of the Input DC Capacitors," in *IEEE Transactions on Industrial Electronics*, 2024.

[16] K. Jena, N. K. Dewangan, R. P. Gupta and D. Kumar, "Transformer-less Switched-Capacitor Inverter for PV Application," *2023 3rd International Conference on Emerging Frontiers in Electrical and Electronic Technologies (ICEFEET)*, Patna, India, 2023, pp. 1-5.

[17] C. J. Rodríguez-Cortés, J. M. Sosa, P. R. Martínez, G. Vázquez-Guzmán and A. R. López, "Overview on Leakage Current Reduction Methods in Single-Phase Grid-Connected Inverters," *2023 IEEE International Autumn Meeting on Power, Electronics and Computing (ROPEC)*, Ixtapa, Mexico, 2023, pp. 1-6.

[18] C. C. A. De Carvalho, P. R. D. R. Da Silva, J. A. Pomilio and J. M. Araújo, "Leakage Current Mitigation in Transformerless Grid-Connected PV Inverters Through Level Modulation Switching," *2023 IEEE 8th Southern Power Electronics Conference and 17th Brazilian Power Electronics Conference (SPEC/COBEP)*, Florianopolis, Brazil, 2023, pp. 1-7.

[19] M. Biswas, S. P. Biswas, S. Mondal, A. B. Islam, M. Rabiul Islam and A. Fekih, "A High Performance Switched-Capacitor Based Single-Phase Transformerless Inverter," *2023 IEEE International Conference on Applied Superconductivity and Electromagnetic Devices (ASEMD)*, Tianjin, China, 2023, pp. 1-2.

[20] A. R. A. Pinto, F. A. C. Bahia, R. P. R. Souza, J. R. Pinheiro and F. F. Costa, "Single-Phase Transformerless UPS with Interleaved Boost Converters for Battery Discharging," *2023 IEEE Energy Conversion Congress and Exposition (ECCE)*, Nashville, TN, USA, 2023, pp. 1487-1493.

[21] A. Gangwar, N. Deshmukh, A. Chanekar and S. Anand, "Highly Efficient GaN-Based PV Inverter with Reduced Leakage Current," *IECON 2023- 49th Annual Conference of the IEEE Industrial Electronics Society*, Singapore, Singapore, 2023, pp. 1-6.

[22] R. A. Mastromauro, "Analysis of Performances of Single-Phase PV Transformer-Less Inverters for Compliance with the New Standards CEI 0-21and IEEE 1547-2018," *2023 IEEE 17th International Conference on Compatibility, Power Electronics and Power Engineering (CPE-POWERENG)*, Tallinn, Estonia, 2023, pp. 1-6.

[23] F. Akbar, M. Elgenedy, A. Elkhateb, H. Cha and J. -W. Park, "Novel Virtual-Ground Single-Phase Buck-Boost Inverter," *2023 11th International Conference on Power Electronics and ECCE Asia (ICPE 2023 - ECCE Asia)*, Jeju Island, Korea, Republic of, 2023, pp. 544-548.

[24] E. Demirkutlu and I. Iskender, "A Novel Transformerless Single-Phase Three-Level Buck-Boost Inverter," *2023 IEEE Applied Power Electronics Conference and Exposition (APEC)*, Orlando, FL, USA, 2023, pp. 114-120.